

Article

Multiscale and Multi-Technical Approach to Characterize the Hot-Dip Galvanized Steel Surface and Its Consequence(s) on Paint Adhesion and Tendency to Blistering

Krystel Pélissier *  and Dominique Thierry 

French Corrosion Institute, 220 Rue Pierre Rivoalon, 29200 Brest, France; dominique.thierry@institut-corrosion.fr

* Correspondence: krystel.pelissier@institut-corrosion.fr

Abstract: It is well known that the surface state (cleanliness, composition) of galvanized steel prior to the application of an organic coating is an important parameter. The surface state will affect the adhesion properties of the complete system and therefore will also impact its corrosion resistance and its tendency to blistering. Before the application of a pretreatment layer, galvanized steel strips are normally alkaline cleaned. This step is known to remove the native oxide film formed on hot dip galvanized steel after processing and appears as one of the most important steps to study the impact of the surface properties on the performance of painted systems. This study focused on making use of the cleaning step to input a variability on the surface composition (mainly surface concentration of aluminum) and evaluate its consequence(s) on the performance of a complete paint system. The results showed that, a variability in terms of surface aluminum concentration could be achieved by the cleaning step and that signs of performance improvement in terms of adhesion and tendency to blistering were spotted with a low content of aluminum at the surface.

Keywords: alkaline cleaning; surface characterization; hot-dip galvanized steel; paint adhesion; blistering



Citation: Pélissier, K.; Thierry, D. Multiscale and Multi-Technical Approach to Characterize the Hot-Dip Galvanized Steel Surface and Its Consequence(s) on Paint Adhesion and Tendency to Blistering. *Coatings* **2021**, *11*, 704. <https://doi.org/10.3390/coatings11060704>

Received: 16 May 2021
Accepted: 9 June 2021
Published: 11 June 2021

Publisher's Note: MDPI stays neutral with regard to jurisdictional claims in published maps and institutional affiliations.



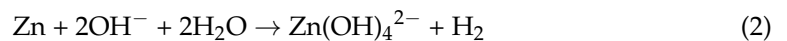
Copyright: © 2021 by the authors. Licensee MDPI, Basel, Switzerland. This article is an open access article distributed under the terms and conditions of the Creative Commons Attribution (CC BY) license (<https://creativecommons.org/licenses/by/4.0/>).

1. Introduction

Due to a small addition of aluminum (0.1–0.3 wt%) in the galvanizing bath, to its limited solubility in zinc matrix, and to its affinity to oxygen, the surface of hot-dip galvanized steel (HDG) is enriched in aluminum. An atomic concentration ratio of Al to Zn of about 1–3:1 for the uppermost 30 Å was observed by Feliu et al. [1] on HDG and Galfan (Zn–5Al) surfaces and the presence of a thin film of aluminum oxide at the extreme surface is now well accepted and documented [1–9].

It is well known that the surface state of galvanized steel prior to the application of a coating is an important parameter. Early work performed by Kim and Leidheiser in the 1970s tried to assess the effect of the surface composition of HDG strips on paint adhesion [10,11]. By coupling surface characterization (Auger electron spectroscopy) to paint adhesion measured by the deformation test (wedge bend test, the O-T-bend test), they showed that the ability of HDG to retain paint deformation was at its maximum when low residuum of carbonaceous material and aluminum involved in the native oxide film at the surface were measured [10]. In addition, to affect the adhesion properties of the complete system, the surface state of HDG steel will also impact its performance related to corrosion resistance and its tendency to blistering. Recent studies have highlighted the impact of the distribution of the pretreatment layer on the tendency to blistering and were able to partially link it to the presence of the native aluminum oxide film at the surface [12–17]. Furthermore, studies have shown, that in the case of phosphate-based and chromate-based conversion layer, the presence of the native aluminum oxide film at the surface could delay the formation of the conversion layer and thus reduce its thickness [2,4,16,18]. Indeed, they demonstrated that before being able to begin the dissolution-precipitation process

forming the conversion layer, the solution of the conversion coating needed to dissolve any remaining aluminum at the surface. Usually, before application of a pretreatment layer, HDG steel strips are alkaline cleaned. This step is performed to remove any contamination at the surface, such as oils, to improve the wettability of the surface and is also known to dissolve aluminum phases and remove the native oxide film [6,8,13,19,20]. Indeed, the hydroxide ions in the etchant react with the metal-oxide surface and cause the dissolution of the oxide layer and the underlying metal. The following reactions can be used to describe the dissolution [6]:



By generating a surface predominant in zinc compounds and with reduced levels of aluminum and carbon, the cleaning step appears as one of the most important steps in controlling the amount of aluminum at the surface and to study the impact of the surface properties on the performance of painted systems.

This study presents a new approach to change the surface chemistry of HDG steel using the cleaning step to input a variability on the surface composition (mainly the surface concentration of aluminum) and evaluate its consequence(s) on the performance of a complete paint system by means of laboratory testing. Therefore, the surface of HDG steel was tuned by alkaline cleaning, characterized by means of high depth resolution tools and laboratory coated. Then, their performance in terms of adhesion and resistance to blistering were examined with traditional means (T-bend test and continuous condensation test).

2. Materials and Methods

2.1. Materials

Temper rolled HDG material obtained from a continuous galvanizing line ($\approx 0.2\%$ Al in the zinc bath) with a total coating mass of 275 g/m^2 on both sides and with a thickness of 0.5 mm was used.

2.2. Cleaning Process and Paint Application

All samples were cleaned with a typical KOH-based alkaline cleaning solution at different pH values ranging from about 8 to 13. One should note that although the pH was varied, the same chemistry was used for the cleaning solution (e.g., KOH) to limit any potential changes in the surface composition which could arise from the use of cleaning solutions with different chemistries. A near neutral pH (8) cleaning solution was chosen to reach an oil-free/Al-rich state, a medium (10–12) and a high alkali one (>13) to obtain two partly Al-free states with different contents of aluminum remaining at the surface. The different pH values were selected based on internal data.

For surface characterization measurements, samples were first ultrasonically solvent cleaned in Heptane during $2 \times 15 \text{ min}$ to remove oil and other contaminants. This step was added to achieve the same surface state before alkaline cleaning. It should be noted that the solvent cleaned samples without further alkaline cleaning served as reference in this work.

From the study by Berger et al. [6], it is known that both the time and the temperature of the cleaning step are important parameters to select. For this study, it was decided to clean the samples at $50 \text{ }^\circ\text{C}$, for the alkaline cleaners with a $\text{pH} \approx 10$ and a $\text{pH} > 13$, which is a temperature close to real conditions of cleaning for coil coating materials [5,12]. As the near neutral cleaner ($\text{pH} = 8$) was chosen to reach an oil free/Al-rich state, a temperature of $40 \text{ }^\circ\text{C}$ was selected to avoid too much etching and at the same time obtain a correct cleaned state. Thus, HDG samples were alkaline cleaned by dipping at 40 or $50 \text{ }^\circ\text{C}$ (as a function of the pH of cleaner) with various times of exposition. Then, the samples were rinsed in deionized water and dried in air.

For laboratory testing (blistering and adhesion tests), the substrates were cleaned using a typical spray cleaning machine ($9.6 \text{ mL/cm}^2/\text{min}$) (Technowash, Northallerton, UK). All solutions were used at a concentration of $20 \text{ g}\cdot\text{L}^{-1}$.

The alkaline cleaned samples were coated with a pretreatment primer with an acrylic based chemistry which combined the pretreatment and the primer layer in one single layer ($\sim 5 \text{ }\mu\text{m}$ layer) [21]. Then, a polyester topcoat Dynapol LH 830 (open source topcoat from Evonik) was applied ($\sim 20 \text{ }\mu\text{m}$ layer). The primer and the topcoat were applied with a barecoater.

2.3. Surface and Interface Characterization

2.3.1. Topography Measurements

An optical profiler Wyko 1100 NT (Veeco, Dourdan, France) has been used to measure the surface topography of HDG steel. The topography measurements have been carried out at three different locations on a $1.2 \times 0.9 \text{ mm}^2$ area. These measurements were focused on the average roughness, R_a , which is the arithmetic mean of the absolute departures of a roughness profile from the mean line of measurements as depicted in [22]. The average roughness is expressed in micrometers and is the most universally recognized and used international roughness measurements.

2.3.2. Raman Spectromicroscopy

Raman measurements were carried out using a confocal Raman spectrometer Horiba-Jobin Yvon Xplora Plus (Horiba France SAS, Palaiseau, France) equipped with a TE-cooled CCD camera (1024×256 pixels). A 532 nm laser source was used with a $\times 100$ objective and a 1200 grooves per mm grating. Several areas were analyzed, up to 5, and the spectrum presented is representative of the spectral signature obtained.

2.3.3. X-ray Photoelectron Spectroscopy (XPS)

XPS spectra were obtained using a KRATOS NOVA X-ray photoelectron spectrometer (Kratos Analytical Ltd, Manchester, UK) with a monochromatised $\text{AlK}\alpha$ X-ray ($h\nu = 1486.6 \text{ eV}$). Survey scans were used to determine the chemical elements. They were acquired with an analyzer pass energy of 160 eV. The elemental composition was obtained using the survey scan with 10 times more point than usual to obtain a better quantification. High resolution spectra of oxygen (O1s) were acquired with an analyzer pass energy of 20 eV and a step of 0.1 eV. The size of the analyzed area was $300 \times 700 \text{ }\mu\text{m}^2$ and two replicates were analyzed.

2.3.4. Glow Discharge Optical Emission Spectrometry (GD-OES)

GDOES was performed using a LECO GDS 850 A (LECO Technik GmbH, Schönsee, Germany). By means of calibration with reference materials (RM) and certified reference materials (CRM), the depth profiles are quantified to mass or atomic fractions vs. depth.

2.3.5. Electrochemical Impedance Spectroscopy (EIS)

Electrochemical impedance spectroscopy measurements were carried out in a water electrolyte on the base of de-ionized water containing 1% of NaCl using a Gamry 600 potentiostat (Gamry Instruments, Warminster, PA, USA). A saturated calomel electrode was used as a reference electrode and a stainless-steel cell served as a counter electrode. The measurements were performed at 20 mV voltage perturbation within a frequency range from 100 to 0.01 Hz. The samples were exposed to the electrolyte up to 30 days and the monitoring was performed since the start of the exposure. The low-frequency data were extracted at 0.1 Hz. This analysis was repeated once.

2.4. Laboratory Tests

2.4.1. Humidity Resistance Testing

An indication of the paint performance in relation to its tendency to blistering was obtained with a water condensation (QCT) test at 60 °C. According to ASTM D 4585 [23], ISO 6270 [24] or ASTM D2247 [25], the test should be conducted at 40 °C. However, better correlation to the extent of blistering in marine field atmosphere have been obtained when the test is conducted at 60 °C [26]. Three painted samples were exposed and inspected after 500 and 1000 h. The extent of blistering was evaluated following ISO 4628-2 [27]. In addition, the panels were evaluated according to an internal ranking system described in Table 1. This internal ranking enabled numerical processing of the results.

Table 1. Internal ranking of blistering with approximate correlation to the ISO 4628-2 [27] rating.

Ranking	Description	ISO 4628-2				
		S1	S2	S3	S4	S5
1	Free of blisters	-	-	-	-	-
2	Several very small blisters	2S1	1S2	-	-	-
3	Low extent of blistering	3S1	2S2	1S3	1S4	-
4	Blistering	4S1, 5S1	3S2, 4S2	2S3, 3S3	2S4	-
5	Heavy blistering	-	5S2	4S3	3S4	1S5, 2S5
6	Dramatic blistering	-	-	5S3	4S4, 5S4	3S5, 4S5, 5S5

2.4.2. T-Bend Testing

The T-bend test was used to assess the dry adhesion of the different painted systems according to ASTM D4145 [28]. Paint de-adhesion and cracking was evaluated after bending of 80 × 35 mm² strips at 0, 0.5, 1, and 1.5 T. Again, the panels were evaluated according to an internal ranking to enable numerical processing of the results, see Table 2. When the loss of adhesion was too severe it was impossible to evaluate cracking.

Table 2. Internal ranking for the T-bend test.

Classification	Adhesion	Cracking
1	No loss of adhesion	No cracking
2	No loss of adhesion	Cracking
3	Slight loss of adhesion: Less than 10% of the bend area delaminated	No cracking
4	Slight loss of adhesion: Less than 10% of the bend area delaminated	Cracking
5	Loss of adhesion: At least 10% of the bend area delaminated	Not assessed
6	Severe loss of adhesion: >50% of the bend area delaminated	Not assessed

2.4.3. N-Methyl Pyrrolidone (NMP) Test

The NMP used was a p.a. chemical. NMP is a highly polar solvent and can form strong hydrogen bonds which allow it to rapidly diffuse into organic coating causing extensive swelling. Due to the swelling, shear stresses are imposed at the metal-coating interface and are relaxed by delamination of the coating. The longer the time until delamination, the better the adhesion. In the NMP delamination test, panels of 4 cm² area were immersed in NMP at 60 °C. The coating always delaminated from the edges inwards. The time when the coating had completely come off was recorded (NMP retention time—NMPRT). After 2 h without delamination, the test was stopped.

3. Results and Discussion

3.1. Preparation of Surface with Different Aluminium Concentration

3.1.1. Hot-Dip Galvanized Steel Surface before Alkaline Cleaning

Before evaluating the effect of the alkaline cleaning on the surface of HDG steel, it was important to first characterize it. Figures 1 and 2 show that the surface of HDG after

temper rolling is a rough surface with a plateau-valley morphology enriched in zinc oxide in the valley.

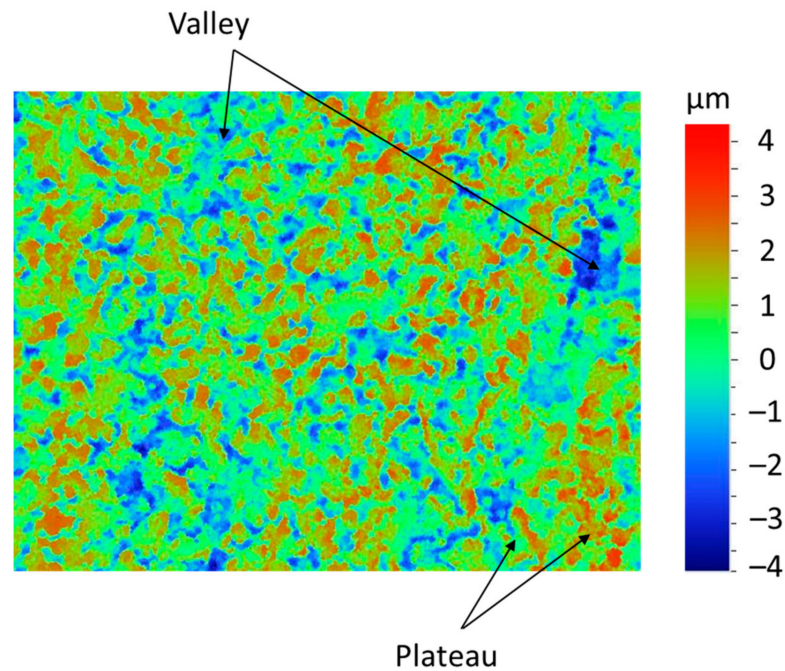


Figure 1. Surface profile for bare HDG steel after solvent cleaning obtained by optical profiler ($1.2 \times 0.9 \text{ mm}^2$).

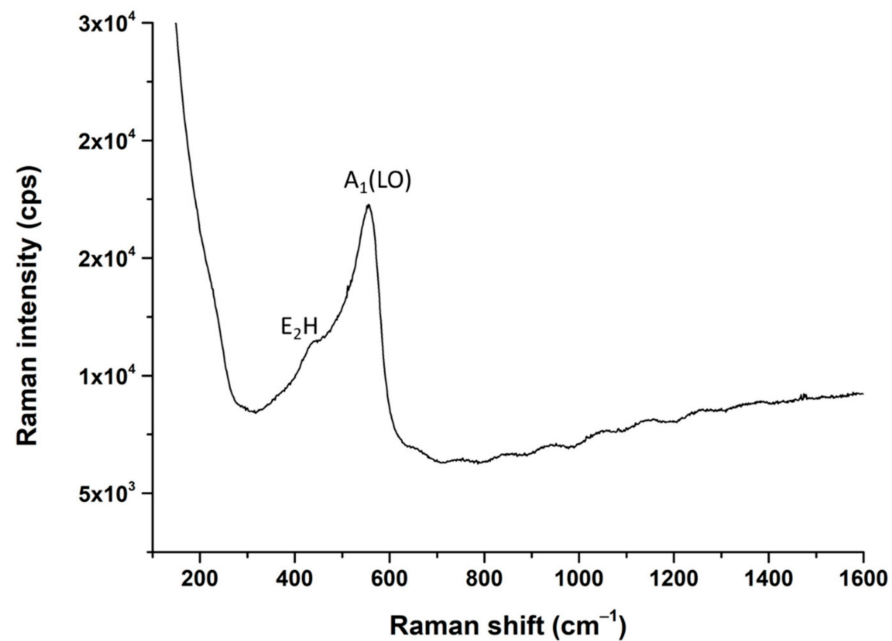


Figure 2. Raman spectra between 100 and 1600 cm^{-1} for bare HDG steel in a valley after solvent cleaning.

Indeed, zinc oxide signals around 560 and 440 cm^{-1} were obtained with Raman spectromicroscopy measurements. Those signals are attributed to the $A_1(\text{LO})$ mode and to the $E_2\text{H}$ mode, respectively and their intensity ratio indicates that the zinc oxide was in an amorphous state [29–33]. The presence of zinc oxide in the valley can be explained by the temper rolling step. This step is known to mechanically break the native oxide film and to

lead to a plateau-valley morphology [5,34]. On the plateau, the native oxide film remains intact, whereas it is broken in the valley leading to an enrichment in zinc oxide.

In addition to Raman spectromicroscopy, XPS analysis was carried out (see Figure 3). The survey scan of the solvent cleaned surface (reference) showed that carbon, oxygen, aluminum, and zinc were the principal elements on the surface.

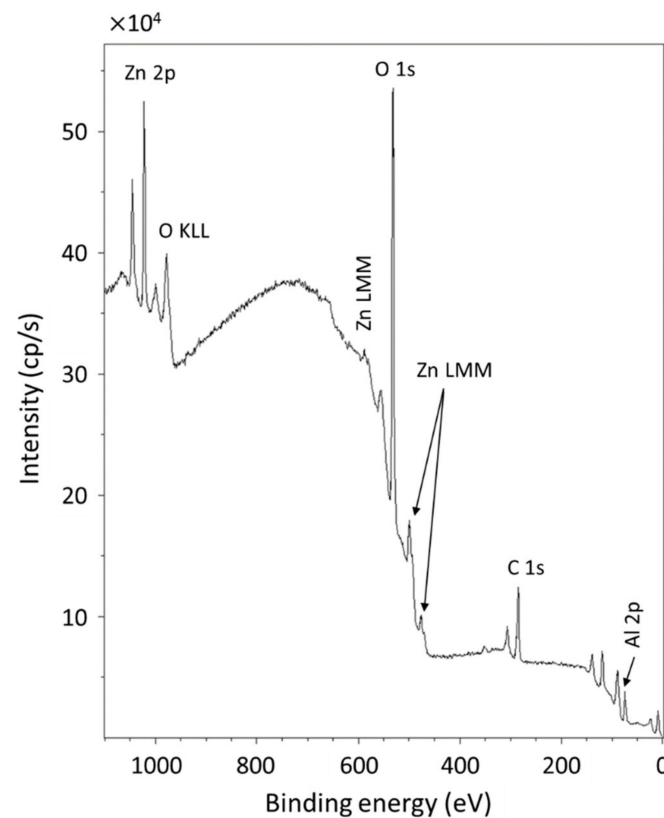


Figure 3. Survey spectrum for bare hot-dip galvanized steel after solvent cleaning obtained by XPS.

The atomic concentration of the different elements is presented in Table 3. The atomic concentration of carbon was low for an industrial surface (around 30%) showing that the solvent cleaning step was successful in degreasing the surface [1]. Oxygen was the most abundant element on the surface showing the oxidized state of the native film.

Table 3. Atomic concentration obtained by XPS of the different elements constituting the surface of bare HDG steel after solvent cleaning.

Elements	C	O	Al	Zn	Al/Zn
[at%]	27.3	49.7	17.3	5.5	3.1

The Al/Zn ratio obtained, i.e., 3.1, is in agreement with the ratio typically found in the literature. Indeed, several studies have shown that the ratio Al/Zn obtained by XPS can vary from 2.5 to 5 after the temper rolling step [1,34,35]. This high variation on the Al/Zn ratio mostly comes from the type of temper-rolling used (random or not random patterns) and the dependence of the concentration of aluminum at the surface with the orientation of zinc grains [36]. In addition to depending on the orientation of zinc grains, the concentration of aluminum at the surface is higher on the plateau where the mechanical solicitation from the temper rolling step is null [5]. Thus, as the area of analysis of XPS can be quite large, i.e., $300 \times 700 \mu\text{m}^2$ in the case of this study, the area will be a mix of plateau and valley signals where the zinc signal is predominant in the valleys and can explain high variations on the Al/Zn ratio.

3.1.2. Study of the Impact of the Time of Alkaline Cleaning

The main focus of this part of this work was to select the correct cleaning conditions to obtain different aluminum concentrations at the surface. It should be noted that this study was focused on the chemical impact of the alkaline cleaning step on the surface of HDG steel. However, the physical impact of this step was still checked, and no influence of the alkaline etching was observed (by roughness measurements or microscopic observations) whatever the pH of the alkaline cleaner or the time of cleaning used. For information, the average roughness for the solvent cleaned, the neutral alkaline cleaner, the mild alkaline cleaner, and the strong alkaline cleaner were 0.95 ± 0.05 , 0.93 ± 0.02 , 0.90 ± 0.01 , and $0.90 \pm 0.02 \mu\text{m}$, respectively.

As it is well-known that only the surface of HDG is enriched in aluminum, the surface sensitive technique such as GD-OES was performed to obtain the depth profile of aluminum on HDG steel for solvent cleaned and alkaline cleaned samples. Only the time of cleaning was varied, and its effect was evaluated using the most alkaline cleaner ($\text{pH} > 13$). It was assumed that if the dissolution of aluminum was only a surface event, it would be easier to highlight it with a most pronounced etching of the surface.

Four times of cleaning were considered (10, 15, 20, and 30 s). The aluminum depth profile obtained by GD-OES for each time and for a solvent cleaned sample is represented in Figure 4.

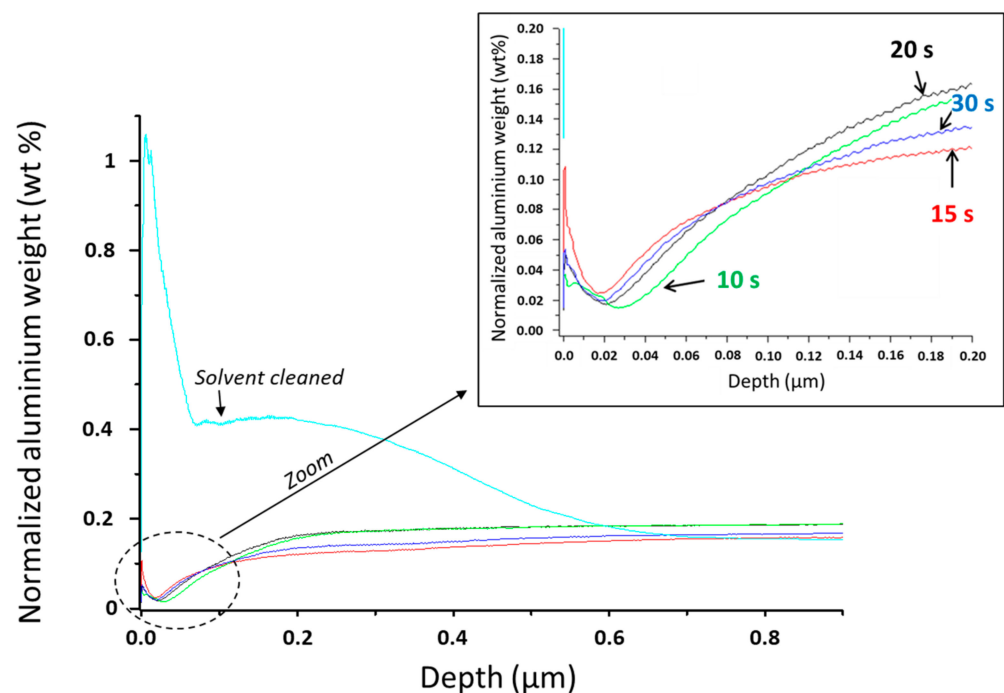


Figure 4. Aluminum depth profile after solvent cleaning (light blue) and after alkaline cleaning (black, green, red, and blue) with the alkaline solution (KOH) $\text{pH} > 13$ (10, 15, 20, 30 s) between 0 and 0.8 μm and between 0 and 0.2 μm (zoom–inset).

As shown in Figure 4, for the solvent cleaned sample, an aluminum enrichment of the first nm ($\sim 100 \text{ nm}$) is present and agrees with the literature [1–9]. After alkaline cleaning, the content of aluminum dropped, and the bulk value was reached after 300 nm. These results are in accordance with the literature showing an aluminum dissolution due to the alkaline cleaning step [6,14–16,37].

It was clearly visible that the depletion of aluminum concentration, represented by the minimum of aluminum weight, happened on the first 50 nm of the surface. A zoom of the first 200 nm, represented in Figure 4, clearly showed that there were no significant

differences between times of cleaning, and at this pH, the aluminum dissolution happened really fast, i.e., after 10 s of cleaning, the aluminum weight was already at its lowest.

Based on these results, it was decided to use a short time of cleaning for all cleaning solutions. The same time of cleaning, i.e., 15 s, was selected to simplify the application process except for the near neutral cleaner (10 s) still in order to reduce the surface etching.

3.1.3. Surface Characterization as a Function of the Alkaline Cleaning Condition

The three different conditions selected above were analyzed by XPS and the atomic composition of the surfaces is reported in Figure 5.

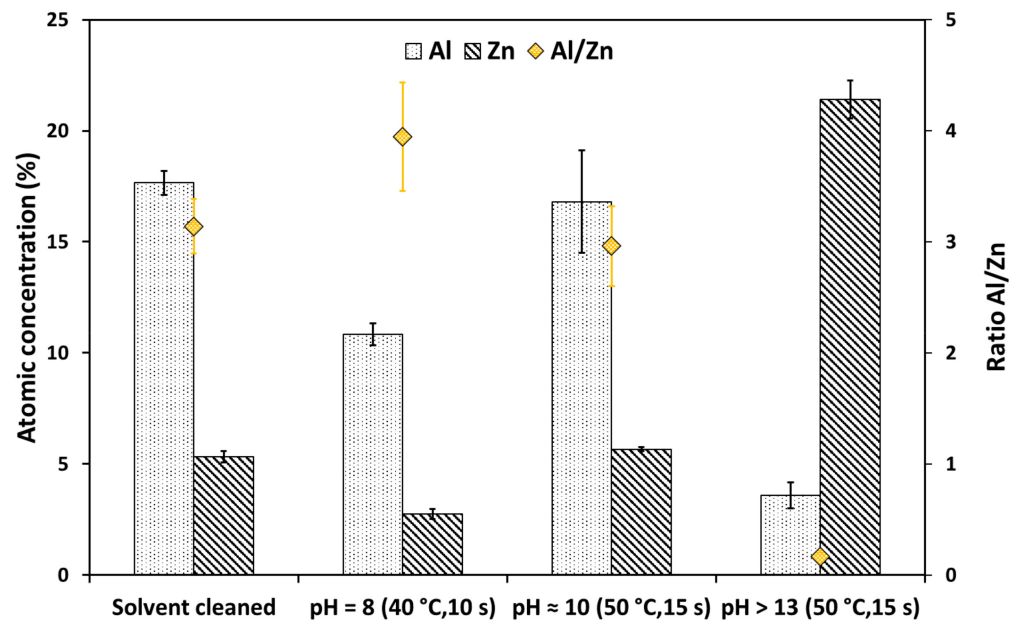


Figure 5. Atomic concentration of aluminum and zinc obtained by XPS on a bare HDG steel after solvent cleaning and alkaline cleaning. The ratio Al/Zn is also plotted.

The ratio Al/Zn will be used to compare the surface cleaned with different conditions rather than only the aluminum atomic concentration since concentrations obtained by XPS are only semi-quantitative. This means that, for example, between two samples a decrease of aluminum atomic concentration would not necessarily be linked to aluminum dissolution but could be linked to an increase of the carbonaceous contamination.

As shown in Figure 5, a clear difference between the reference (solvent cleaned) and the surface cleaned with an alkaline solution (strong solution) was obtained. However, when the neutral cleaner was considered, the Al/Zn ratio appeared higher than the one obtained for the reference (solvent cleaned). This observation could be linked to the variability of the initial surface and the area of analysis. Indeed, if an area with a lot of plateau is analyzed, it can be possible to obtain a higher Al/Zn ratio especially if the etching is low (as desired). Concerning the mild cleaner, the Al/Zn ratio was close to the one observed after solvent cleaning but significantly lower than the one observed for the neutral clear.

For the strong alkaline cleaner (pH > 13), a high enrichment of zinc was visible, and it impacted the composition of the oxide film as shown in Figure 6.

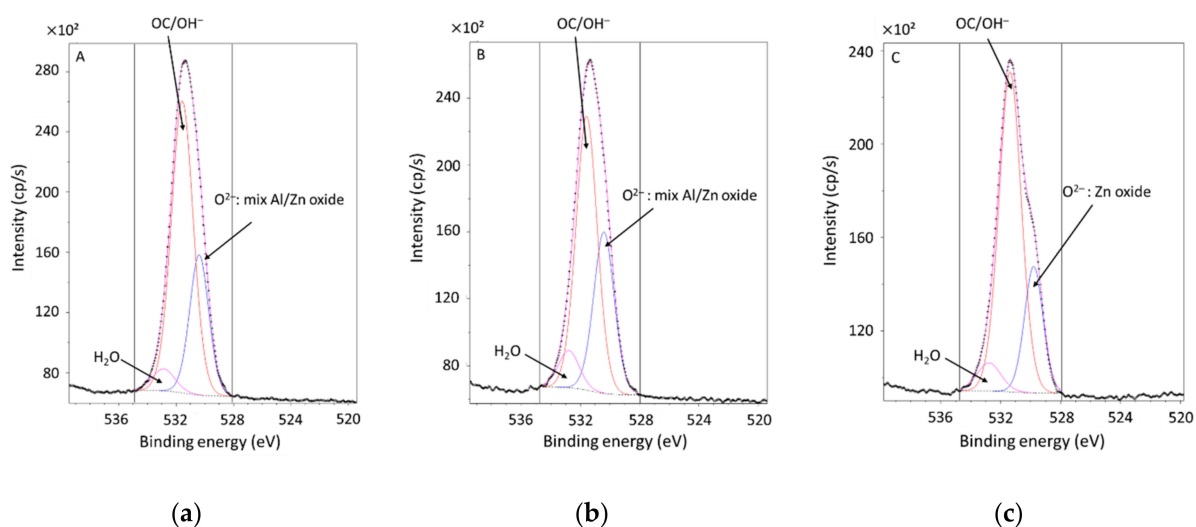


Figure 6. High resolution O1s spectra for bare HDG (a) after solvent cleaning, (b) after alkaline cleaning at 50 °C during 15 s with an alkaline solution at pH \approx 10 and (c) after alkaline cleaning at 50 °C during 15 s with an alkaline solution at pH > 13.

The high-resolution spectra O1s for the solvent cleaned (A), mild alkaline cleaner (B), and strong alkaline cleaner (C) is represented in Figure 6. After cleaning with the strong cleaner, the oxide component (O^{2-}) was shifted to a lower binding energy (-0.6 eV) and the full-width-half-maximum (FWHM) was slightly reduced. This behavior indicated that the oxide film formed after cleaning with the strong alkaline cleaner was mainly composed of zinc oxide [34]. On the other hand, when looking at the shape of the O1s spectrum for the mild cleaner, it was visible that the oxide film at the surface still consisted of a mixed Al/Zn oxide [6].

This part of the study showed that it was possible to obtain distinct HDG surface states with different concentrations of aluminum using the alkaline cleaning step. For the rest of this study, the following conditions will thus be used for alkaline cleaning before the paint application:

- Oil free/Al-rich state: Neutral cleaner at 40 °C during 10 s
- Partly Al free: Mild cleaner at 50 °C during 15 s
- Mostly Al free: Strong cleaner at 50 °C during 15 s

3.2. Effect of Aluminium Concentration on Adhesion and Tendency to Blistering

3.2.1. Study of the Interface Stability in the Presence of Water

In order to study the impact of the cleaning conditions on the interface stability in the presence of water, electrochemical impedance measurements have been carried out. The Bode plots (impedance modulus and phase angle) for each cleaning condition as a function of the exposition to electrolyte are reported in Figure 7.

For the three cleaning conditions, initially, the impedance modulus (Figure 7a,c,e) exhibited a capacitive behavior. On the phase angle Bode plots (Figure 7b,d,f), the phase angle was close to -90° indicating an adherent film. The low-frequency impedance modulus at 0.01 Hz was extracted from the measurements and monitored as a function of the time of exposure for the three cleaning conditions to determine the stability of the metal/paint interface when exposed to the electrolyte (see Figure 8). It is well known that a decrease in the low frequency impedance versus time may reflect of a poor adhesion of the coating.

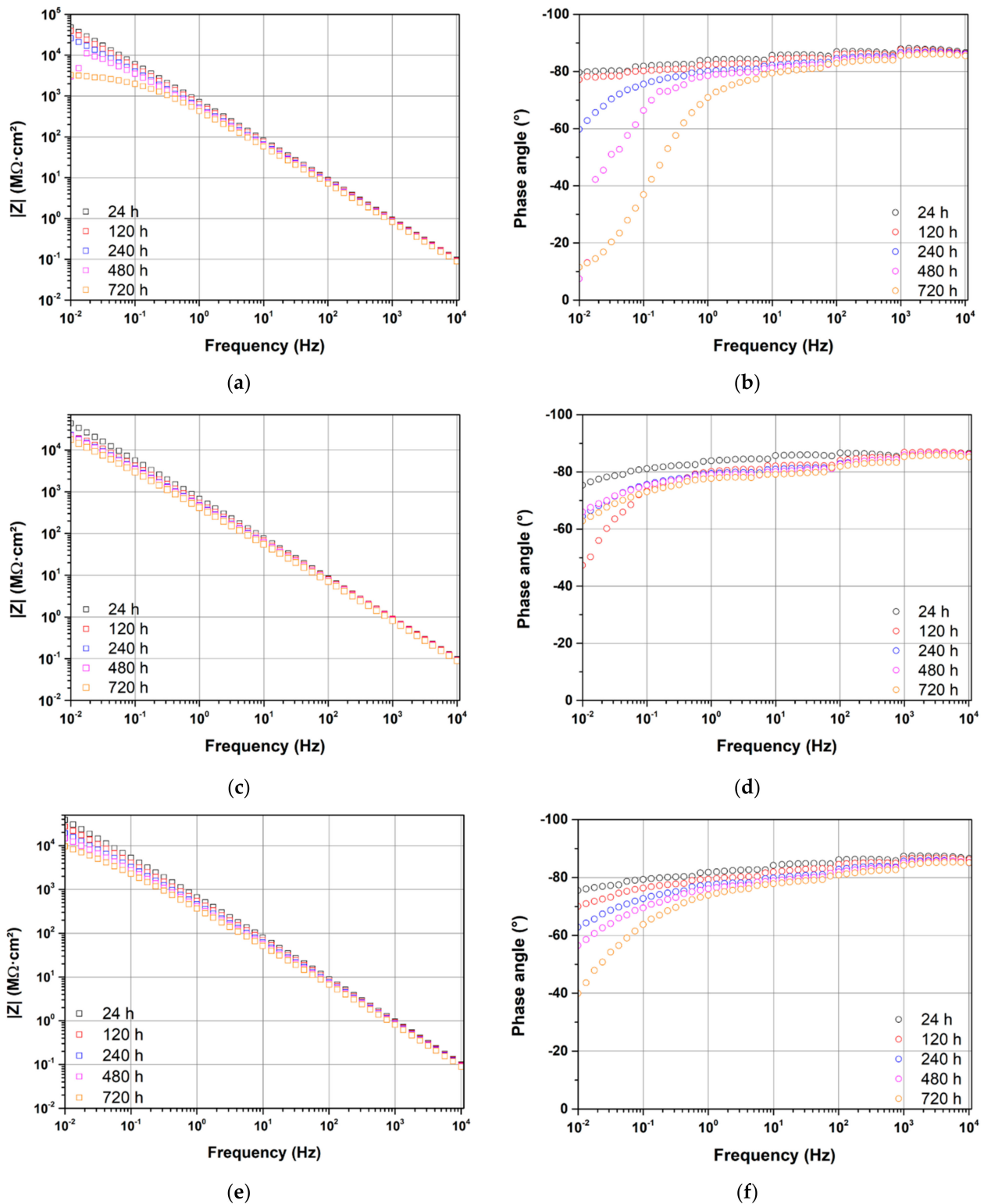


Figure 7. Electrochemical impedance spectra 1% NaCl for painted HDG steel as a function of the time of exposure (a) impedance modulus and (b) phase angle for the neutral cleaner (pH = 8), (c) impedance modulus and (d) phase angle for the mild alkaline cleaner (pH \approx 10), (e) impedance modulus and (f) phase angle for the strong alkaline cleaner (pH > 13).

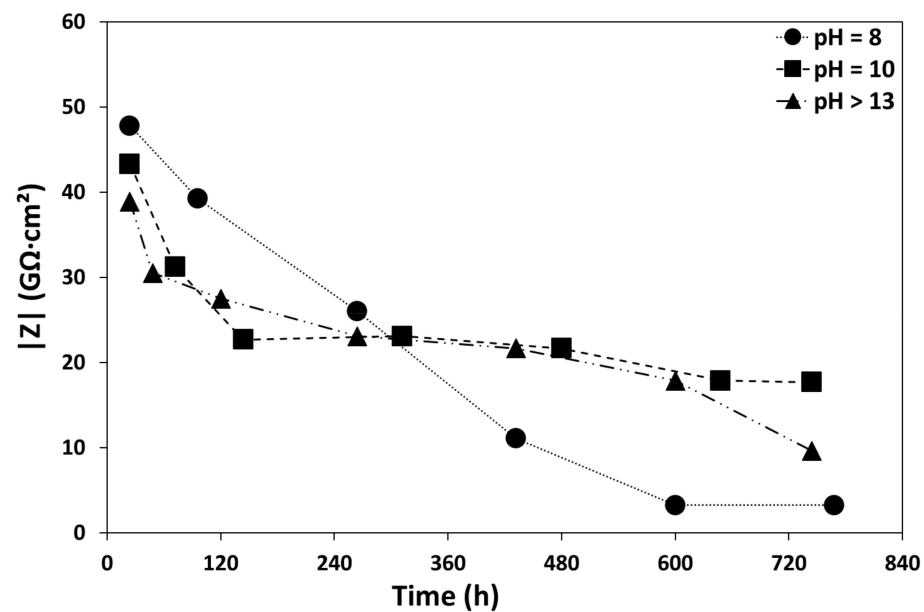


Figure 8. Monitoring of impedance modulus at 0.1 Hz in 1% NaCl for painted HDG steel as a function of the time of exposure and the pH of the alkaline solution (neutral cleaner (pH = 8), mild alkaline cleaner (pH \approx 10) and strong alkaline cleaner (pH > 13)).

Initially (after 1 day of exposure), all samples exhibited a high low-frequency modulus at about $4\text{--}5 \times 10^{10} \Omega\cdot\text{cm}^2$ showing good barrier properties and probably good adhesion independently on the cleaning conditions. Indeed, a low-frequency modulus higher than $10^7 \Omega\cdot\text{cm}^2$ is normally an indicator that the coating provides good corrosion protection [38,39]. The lowest impedance value was found when the metallic surface was cleaned with the near neutral cleaner. Indeed, the low-frequency modulus kept decreasing until 25 days to stabilize at a lower value.

Concerning the other cleaning conditions (pH \approx 10 and pH > 13), a decrease of about 60% and 75% after 31 days of exposure was observed for the mild cleaner and the strong cleaner, respectively. When comparing the two conditions, it seemed that the best interface stability was achieved with the mild cleaner. It should be noted that, even though the low-frequency modulus was significantly reduced for all conditions, the paint system still retained enough protective ability at the time scale of this experiment, i.e., 30 days. As seen in Figures 7 and 8, a reduced Al surface content appeared to be beneficial in terms of the interface stability when exposed to the water electrolyte at ambient temperature and at the time scale of this experiment. This improvement of the water stability could be linked to a stronger interface between the pretreatment primer layer and the surface. Indeed, when exposed to water or electrolyte, the bonds between the metal and the organic molecules can be weakened by water. This weakening can be due, according to Leidheiser and Funke [40], either to a chemical disbondment or to a mechanical (hydrodynamic) disbondment. For the first one, it implies that water molecules can disrupt the interactions between the coating and the surface in the case where the interactions are secondary interactions such as acid-base, Van der Waals interaction or hydrogen bonding. In the second case, the loss of adhesion is attributed to the accumulation of water at the interface which induces swelling and internal stress. If the presence of remaining native aluminum oxide on the surface hindered the correct formation of the pretreatment layer as depicted in the literature [8,12–17], it can be supposed that it can lead to an incomplete layer and thus to a weaker interface with reduced stability towards water. In addition, the native aluminum oxide on the surface of HDG steel is known to be inert and to form weaker bonds towards organic molecules [2,8,12,14,41].

3.2.2. Paint Performance: Adhesion and Resistance to Blistering

In addition to the EIS experiment, macroscopic evaluations of the effect of the aluminum concentration at the surface was carried out with the T-bend test and QCT test. The T-bend test is a well-known adhesion test performed in the coil-coating industry. It is designed to test the coating flexibility and capacity to retain good adhesion during additional forming steps. This test depends on the thickness of the substrate and coating, the flexibility of the coating, and its tendency to crack. Normally, it is not recommended to compare the coating with the different chemistry nature, but it is indicated for this study that the substrate, the pretreatment primer, and the topcoat are the same for all samples as only the surface state was varied.

Results of the T-bend test are presented in Figure 9. Only the results for the 1.5 T-bend are shown since high degradation was visible for the more severe bends (1, 0.5, and 0 T) with no significant differences between cleaning conditions. Hence, the loss of adhesion was high with no possibilities to evaluate the appearance of cracks.

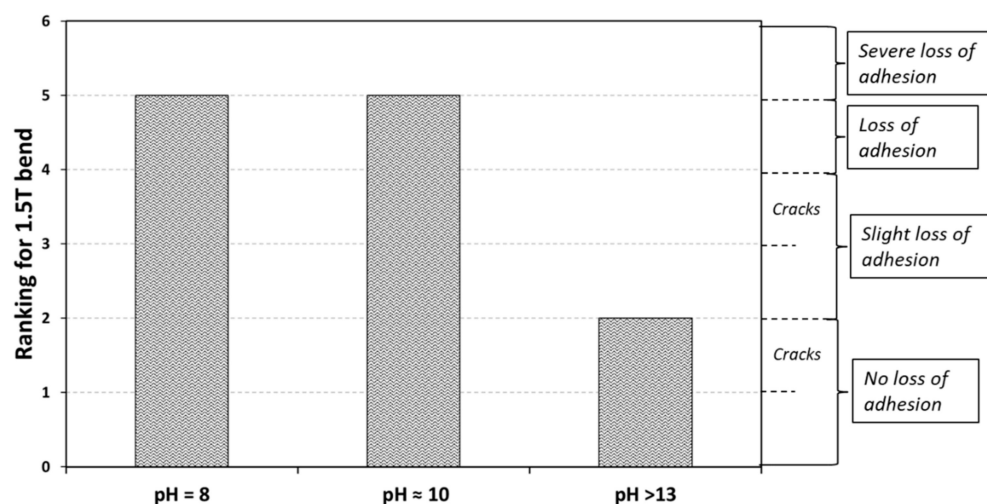


Figure 9. Ranking for the 1.5 T test for painted HDG steel as a function of the conditions of alkaline cleaning.

When analyzing more thoroughly the results for the 1.5 T-bend, a slight improvement of the performance for the condition with the higher pH, i.e., pH > 13, can be seen. For the mild and the near neutral cleaner, no obvious differences were seen in terms of performance. These results tended to show that a lesser extent of aluminum at the surface was beneficial in terms of dry adhesion which is coherent with the literature even though this improvement was rather discrete [11]. Greunz et al. [42] in their work showed that the substrate pretreatment could induce significative differences in the response obtained by the T-bend test. However, when comparing the solvent and alkaline cleaned samples, they only observed small differences which is coherent with the result obtained in this work. To confirm the impact of the alkaline cleaning on adhesion, a physicochemical measurement of adhesion in a dry state was performed by dipping samples in the NMP solvent. As explained in the experimental part, NMP is a highly polar solvent capable of forming strong hydrogen bonds and leading ultimately to the delamination of the coating through its diffusion at the interface [43]. Good adhesion is translated by a longer time to delamination. The results obtained for the different conditions of alkaline cleaning are reported in Table 4.

Table 4. Time to delamination in the NMP solution for the painted HDG steel as a function of the conditions of the alkaline cleaning.

Cleaning Conditions	NMPRT (s)
pH = 8	332 (± 138)
pH \approx 10	255 (± 137)
pH > 13	No delamination observed after 2 h of test

Even though no clear difference in terms of adhesion was spotted between the neutral and the mild cleaner, a clear improvement of the adhesion when the surface was alkaline cleaned with the strong cleaner (pH > 13) was seen as no delamination was obtained after 2 h of immersion in the NMP. In addition, Raman spectromicroscopy measurements carried out on failure locus showed that the failure occurred between the surface and the pretreatment primer layer ruling out a failure between the primer and the topcoat. Those results showed that this improvement was due to a stronger interface between the surface and the paint system.

These results confirmed that a lesser extent of aluminum at the surface was beneficial in terms of adhesion. From a pure adhesion point of view, the improvement of the adhesion with a low concentration of aluminum at the surface could be explained by the inert behavior of the native oxide film on the surface after the galvanizing process [2,8,12,14]. According to the literature, the native oxide film is composed of γ -Al₂O₃ or amorphous aluminum oxide and it is known that for adhesion, the hydroxide form and most particularly the hydroxyl fraction are beneficial in particular for aluminum [2,43–45]. Indeed, Van den Brand et al. [43] tested the impact of different surface treatments on aluminum surfaces on their adhesion with an epoxy coating and observed that the formation of a pseudo-boehmite layer at the surface led to the improved adhesion. This improvement was due to the formation of a larger number of hydrogen bonds between the surface and the epoxy coating and to a better mechanical anchoring caused by the porous structure of the pseudo-boehmite layer. Furthermore, in another work by Van den Brand et al. [46] still on the surface treatment of aluminum, they showed that the acid-base properties of aluminum surface were dependent on the nature of the oxide and hydroxide at the surface leading potentially to a different reactivity.

In addition, even if exposed to air, aluminum oxide reacts rapidly with the moisture of the air and forms surface hydroxyl, it can also adsorb small organic contaminants and water which can be a hindrance to the adhesion of organic molecules [47]. Thus, it is possible that a lower reactivity of the native aluminum oxide film could lead to a weaker interface.

From a reactivity point of view towards the pretreatment primer layer, it was possible that the lowered adhesion with a higher content of aluminum at the surface could be linked to a lack of reactivity of the surface during the pretreatment process leading to fewer adhesion sites. Indeed, it was shown by Saarima et al. [8,12] that the reactivity of the HDG surface was lowered by the presence of native aluminum oxide at the surface. In addition, most of the pretreatment layer formation on HDG steel relies on their reactivity towards zinc as their formation mechanism goes through a dissolution-precipitation process [4,14–16]. Thus, as the presence of native aluminum oxide at the surface of HDG steel can slow down the formation of the pretreatment layer, it is possible that an incomplete (in thickness or structure) pretreatment layer could result in lowered adhesion.

Results of the QCT test after 500 and 1000 h in terms of the extent of blistering are given in Figure 10.

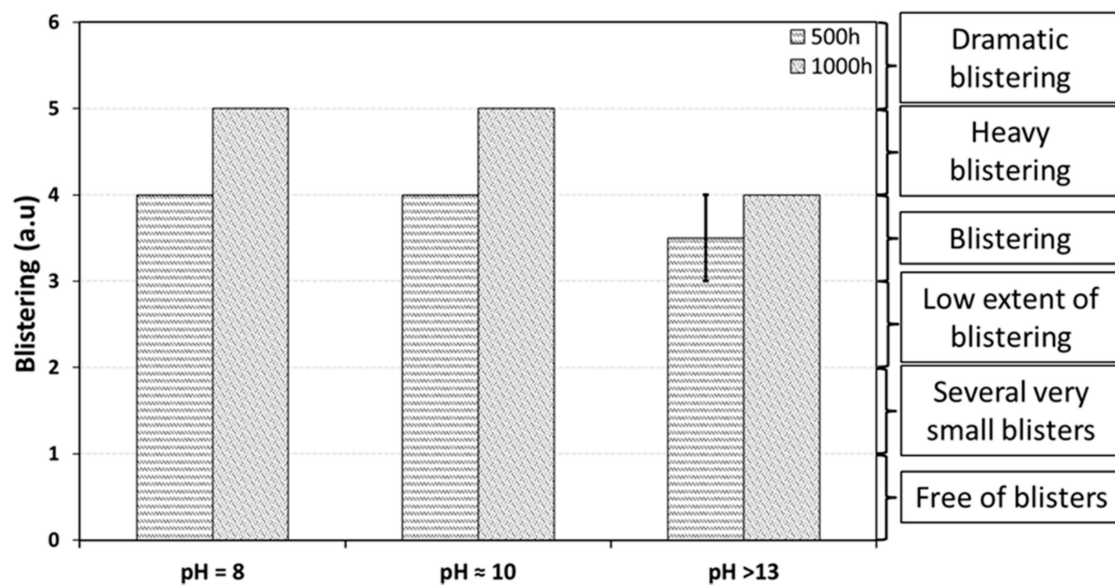


Figure 10. Extent of blistering after QCT for the painted HDG steel as a function of the conditions of alkaline cleaning (3 samples per condition).

The blisters size varied between S1 and S5 as depicted is ISO 4628-2 standard [27], from 1 mm to 4 mm respectively (S5 blisters being localized). In general, the blisters were small but an important quantity. Based on the electrochemical measurements, one would expect a better resistance as the interface appeared more stable in the presence of electrolyte at least after 500 h of test (≈ 20 days). Indeed, some correlation between impedance measurements and blistering appearance has been found [21]. One explanation could come from the difference in the temperature of testing, i.e., ambient temperature for EIS and 60 °C for QCT. Even though the time scale for the degradation was nearly the same when considering 500 h of test, the degradation of the interface could be accelerated at a higher temperature due to its influence on the water transport and paint property [48]. Concerning the effect of the cleaning conditions, cleaning the surface with a strong alkaline cleaner slightly improved the resistance to blistering.

The important quantity of blisters for all conditions and thus the consequent loss of adhesion could be linked to the homogeneity of the pretreatment primer layer. In this work, the pretreatment primer layer is based on a Cr-free chemistry, and it is known that the homogeneity of such a layer is of utmost importance for its protective ability [11–16]. Indeed, Cr-free pretreatments do not have a self-healing ability and rely mostly on a barrier type of protection. As the presence of the inert native aluminum oxide is known to impede the formation of a protective pretreatment layer, it was possible that the performance obtained in the QCT was linked to the inhomogeneity induced by the presence of any remaining inert aluminum native oxide film [8,11–17]. According to Saarimaa et al. [12], an inhomogeneous distribution of the pretreatment layer can promote the absorption of water and oxygen through the pore of the coating by the increased reactions occurring between anodic and cathodic sites created by their inhomogeneity.

It should also be noted that an inhomogeneity of the pretreatment layer on the surface, mostly free of aluminum leading to important blistering during a humidity test, was also observed [12]. This inhomogeneity was linked to the application process of the pretreatment layer which was not optimized. Thus, it was also possible, in the case of this work, that the application process in laboratory conditions did play a role in the performance of the painted systems, as an important quantity of blistering was also observed for the surface with the lesser extent of the remaining aluminum.

From the results concerning the paint performance, it was difficult to conclude firmly on the impact of the aluminum concentration. Indeed, even though, an improvement of the paint performance with the most alkaline condition was observed in terms of adhesion for

the NMP test, the behavior of the paint system was not indisputably distinct upon different cleaning conditions when considering results from the T-bend test and the blistering test. Two hypotheses could be suggested to explain these observations. One could be linked to the fact that the cleaning conditions selected were not sufficient to induce a significant change in the paint system performance despite a clear microscopic impact seen by surface characterization. The other could be linked to the fact that the impact of the surface state was negligible on the performance of the paint systems as the performance of the system appeared poor. Indeed, a high degradation was observed whatever the test considered. In all cases, this type of study proved to be difficult to conduct as it clearly depends on several parameters which can be hard to control. For example, the application process appears of clear importance for the resistance to blistering. Furthermore, even though the lowering of the aluminum surface concentration is known to be beneficial for adhesion between the polymer and the metallic surface, adhesion is not the only parameter to take into account when considering the paint system performance.

4. Conclusions

The surface chemistry of hot-dip galvanized steel samples was tuned by alkaline cleaning with different pH solutions (pH = 8, pH \approx 10, pH > 13). After a thorough characterization to confirm the impact of the cleaning step on surface concentration of aluminum, the samples were laboratory coated. Then, their performance (adhesion and resistance to blistering) was assessed. From those results, the following conclusions may be drawn:

- The use of the cleaning step was found to be a good approach to input variability on the surface when considering the concentration of aluminum at the surface and a solid methodology was developed.
- It was demonstrated that a low content of aluminum at the surface led to a performance improvement when considering adhesion and blistering.
- The impact of the cleaning step, thus the presence of aluminum on the surface, was demonstrated by EIS measurements and the NMP test in dry conditions. Indeed, it was shown that a reduced content of aluminum at the surface gave the best results in terms of interface stability.

This study demonstrated the importance of the cleaning step and the surface state of HDG steel on adhesion and the performance of painted HDG. It also highlighted the difficulty to carry such types of study and to link adhesion to coil performance.

This study also showed that controlling the alkaline cleaning step is of utmost importance during the application process.

Author Contributions: Conceptualization, K.P.; methodology, K.P.; validation, D.T.; formal analysis, K.P.; investigation, K.P.; writing—original draft preparation, K.P.; writing—review and editing, K.P. and D.T.; visualization, K.P.; supervision, D.T.; project administration, D.T. Both authors have read and agreed to the published version of the manuscript.

Funding: This research received no external funding.

Institutional Review Board Statement: Not applicable.

Informed Consent Statement: Not applicable.

Data Availability Statement: Not applicable.

Acknowledgments: Aurélien Renard (LCPME, Nancy) is thanked for the XPS experiments and Dan Persson from Rise for the GD-OES experiments.

Conflicts of Interest: The authors declare no conflict of interest.

References

1. Feliu, S., Jr.; Barranco, V. XPS Study of the surface chemistry of conventional hot-dip galvanized pure Zn, galvanneal and Zn-Al alloy coatings on steel. *Acta Mater.* **2003**, *51*, 5413–5424. [[CrossRef](#)]
2. Maeda, S. Surface chemistry of galvanized steel sheets relevant to adhesion performance. *Prog. Org. Coat.* **1996**, *28*, 227–238. [[CrossRef](#)]
3. Biber, H.E. Scanning Auger Microprobe study of hot-dipped regular spangle galvanized steel: Part I. Surface composition of as-produced sheet. *Metall. Trans. A* **1998**, *19*, 1603–1608. [[CrossRef](#)]
4. Wolper, M.; Angeli, J. Activation of galvanized steel surfaces before zinc phosphating—XPS and GDOES investigations. *Appl. Surf. Sci.* **2001**, *179*, 281–291. [[CrossRef](#)]
5. Puomi, P.; Fagerholm, H.M.; Rosenholm, J.B.; Sipilä, R. Effect of skin pass rolling on the primer adhesion and corrosion resistance of hot-dip galvanized (HDG) steel. *J. Adhes. Sci. Technol.* **2000**, *14*, 583–600. [[CrossRef](#)]
6. Berger, R.; Bexell, U.; Stavlid, N.; Mikael Grehk, T. The influence of alkali-degreasing on the chemical composition of hot-dip galvanized steel surfaces. *Surf. Interface Anal.* **2006**, *38*, 1130–1138. [[CrossRef](#)]
7. Saarimaa, V.; Markkula, A.; Juhanaja, J.; Skirfvars, B.-J. Novel insight to aluminium compounds in the outermost layers of hot dip galvanized steel and how they affect the reactivity of the zinc surface. *Surf. Coat. Technol.* **2016**, *306*, 506–511. [[CrossRef](#)]
8. Saarimaa, V.; Lange, C.; Paunikallio, T.; Kaleva, A.; Nikkanen, J.-P.; Levänen, E.; Väisänen, P.; Markkula, A. Evaluation of surface activity of hot-dip galvanized steel after alkaline cleaning. *J. Coat. Technol. Res.* **2020**, *17*, 285–292. [[CrossRef](#)]
9. Yasakau, K.A.; Giner, I.; Vree, C.; Ozcan, O.; Grothe, R.; Olivieria, A.; Grundmeier, G.; Ferreira, M.G.S.; Zheludkevich, M.L. Influence of stripping and cooling atmospheres on surface properties and corrosion of zinc galvanizing coatings. *Appl. Surf. Sci.* **2016**, *389*, 144–156. [[CrossRef](#)]
10. Kim, D.K.; Leidheiser, H., Jr. Chemistry of the surface of hot-dipped galvanized steel and its relation to paint adherence. *Surf. Technol.* **1977**, *5*, 379–396. [[CrossRef](#)]
11. Leidheiser, H., Jr.; Kim, D.K. Crystallographic factors affecting the adherence of paint deformed galvanized steel. *JOM* **1976**, *28*, 19–25. [[CrossRef](#)]
12. Saarimaa, V.; Kauppinen, E.; Markkula, A.; Juhanaja, J.; Skirfvars, B.-J.; Steen, P. Microscale distribution of Ti-based conversion layer on hot dip galvanized steel. *Surf. Coat. Technol.* **2012**, *206*, 4173–4179. [[CrossRef](#)]
13. Saarimaa, V.; Markkula, A.; Juhanaja, J.; Skirfvars, B.-J. Improvement of barrier properties of Cr-free pretreatments for coil-coated products. *J. Coat. Technol. Res.* **2015**, *12*, 721–730. [[CrossRef](#)]
14. Saarimaa, V.; Markkula, A.; Arstila, K.; Manni, J.; Juhanaja, J. Effect of hot dip galvanized steel surface chemistry and morphology on titanium hexafluoride pretreatment. *Adv. Mater. Phys. Chem.* **2017**, *7*, 28–41. [[CrossRef](#)]
15. Schoeman, L.; Burty, M. Cleaning optimization of hot-dip galvanized steel surfaces in preparation for paint application. *Mater. Sci. Forum* **2018**, *941*, 1772–1777. [[CrossRef](#)]
16. Wilson, B.; Fink, N.; Grundmeier, G. Formation of ultra-thin amorphous conversion films on zinc alloy coatings. Part 2: Nucleation, growth and properties of inorganic-organic ultra-thin hybrid films. *Electrochim. Acta* **2006**, *51*, 3066–3075. [[CrossRef](#)]
17. Zhu, L.Z.; Liang, Y.J.; Yang, J.H.; Chen, X. Investigation on the adhesion improvement of organic coatings on the surface of hot-dip galvanized steel. *J. Phys. Conf. Ser.* **2020**, *1605*, 012128. [[CrossRef](#)]
18. Biber, H.E. Scanning Auger Microprobe study of hot-dipped regular spangle galvanized steel: Part II: Surface composition of chromated sheet. *Metall. Trans. A* **1998**, *19*, 1609–1616. [[CrossRef](#)]
19. Heitbaum, J. New trends in the chemical pretreatment of metal surfaces. *Macromol. Symp.* **2002**, *187*, 43–51. [[CrossRef](#)]
20. Vu, T.N.; Mokaddem, M.; Volovitch, P.; Ogle, K. The anodic dissolution of zinc and zinc alloys in alkaline solution. II. Al and Zn partial dissolution from 5% Al-Zn Coatings. *Electrochim. Acta* **2012**, *74*, 130–138. [[CrossRef](#)]
21. Han, J.; Ogle, K. The anodic and cathodic dissolution of α -phase Zn-68Al in alkaline media. *Corros. Sci.* **2019**, *148*, 1–11. [[CrossRef](#)]
22. Zhang, Y.; Cui, K.; Gao, Q.; Hussain, S.; Lv, Y. Investigation of morphology and texture properties of WSi₂ coatings on W substrate based on contact-mode AFM and EBSD. *Surf. Coat. Technol.* **2020**, *396*, 125966. [[CrossRef](#)]
23. ASTM D4585. *Standard Practice for Testing Water Resistance of Coatings Using Controlled Condensation*; ASTM International: West Conshohocken, PA, USA, 2018.
24. ISO 6270. *Paints and Varnishes—Determination of Resistance to Humidity*; ISO Standard: Brussels, Belgium, 2017.
25. ASTM D 2247. *Standard Practice for Testing Water Resistance of Coatings in 100% Relative Humidity*; ASTM International: West Conshohocken, PA, USA, 2020.
26. Prosek, T.; Nazarov, A.; Stoullil, J.; Thierry, D. Evaluation of the tendency of coil-coated materials to blistering: Field exposure, accelerated tests and electrochemical measurements. *Corros. Sci.* **2012**, *61*, 92–100. [[CrossRef](#)]
27. ISO 4628-2. *Paints and Varnishes—Evaluation of Degradation of Coatings—Designation of Quantity and Size of Defects, and of Intensity of Uniform Changes in Appearance—Part 2: Assessment of Degree of Blistering*; ISO Standard: Brussels, Belgium, 2016.
28. ASTM D 4145. *Standard Test Method for Coating Flexibility of Prepainted Sheet*; ASTM International: West Conshohocken, PA, USA, 2018.
29. Das, J.; Pradhan, S.K.; Sahu, D.R.; Mishra, D.K.; Sarangi, S.N.; Nayak, B.B.; Verma, S.; Roul, B.K. Micro-Raman and XPS studies of pure ZnO ceramics. *Phys. B* **2010**, *405*, 2492–2497. [[CrossRef](#)]
30. Ozgur, U.; Alivov, Y.I.; Liu, C.; Teke, A.; Reschikov, M.A.; Dogan, S.; Avrutin, V.; Cho, S.J.; Morkoç, H. A comprehensive review of ZnO materials and devices. *J. Appl. Phys.* **2005**, *98*, 041301. [[CrossRef](#)]

31. Zhang, Y.; Xie, E. Nature of room-temperature ferromagnetism from undoped ZnO nanoparticles. *Appl. Phys. A* **2010**, *99*, 955–960. [[CrossRef](#)]
32. Sendi, R.K.; Mahmud, S. Quantum size effect on ZnO nanoparticle-based discs synthesized by mechanical milling. *Appl. Surf. Sci.* **2012**, *258*, 8026–8031. [[CrossRef](#)]
33. Aksyanov, I.G.; Kompan, M.E.; Kul'kova, I.V.; Stepanov, Y.P. Luminescence and Raman spectra of sol-gel-derived ZnO microcrystals with a high iron content. *Glass Phys. Chem.* **2012**, *38*, 143–148. [[CrossRef](#)]
34. Mataigne, J.-M.; Vaché, V.; Repoux, M. *Surface Chemistry and Reactivity of Skin-Passed Hot-Dip Galvanized Coating*; Galvatech'07: Osaka, Japan, 2007; pp. 1–6.
35. Guillom, M.F.; Pfister-Guillouzo, G.; Bremont, M.; Brockmann, W.; Quet, C.; Chenard, J.Y. Application of X-Ray Photoelectron spectroscopy to the study of degradation mechanisms of epoxy-bonded joints of zinc coated steel. *Appl. Surf. Sci.* **1997**, *108*, 149–157. [[CrossRef](#)]
36. Vaché, V. *Galvanized Steel Sheets: Deformation, Texture, Ageing, Surface Reactivity*. Ph.D. Thesis, École des Mines de Paris, Paris, France, 2007.
37. Fink, N.; Wilson, B.; Grundmeier, G. Formation of ultra-thin amorphous conversion films on zinc alloy coatings, Part 1: Composition and reactivity of native oxides on ZnAl (0.05%) coatings. *Electrochim. Acta* **2006**, *51*, 2956–2963. [[CrossRef](#)]
38. Lu, F.; Song, B.; He, P.; Wang, Z.; Wang, J. Electrochemical impedance spectroscopy (EIS) study on the degradation of acrylic polyurethane coatings. *RCS Adv.* **2017**, *7*, 13742–13748. [[CrossRef](#)]
39. Lee, C.C.; Mansfeld, F. Automatic classification of polymer coating quality using artificial neural networks. *Corros. Sci.* **1999**, *41*, 439–461. [[CrossRef](#)]
40. Leidheiser, H.; Funke, W. Water disbondment and wet adhesion of organic coatings on metals: A review and interpretation. *J. Oil Colour Chem. Assoc.* **1987**, *70*, 121–132.
41. Gaillard, F.; Peillex, E.; Romand, M.; Verchère, D.; Hocquaux, H. Influence of surface treatments of hot-dip galvanized steels on their acid-base properties and on their reactions with some organic compounds. *Surf. Interface Anal.* **1995**, *23*, 307–312. [[CrossRef](#)]
42. Greunz, T.; Lowe, C.; Schmid, M.; Wallner, G.M.; Strauss, B.; Stifter, D. Dry adhesion study of polyester/melamine clear coats on galvanized steel. *Int. J. Adhes. Adhes.* **2019**, *95*, 1–10. [[CrossRef](#)]
43. Van den Brand, J.; Van Gils, S.; Terryn, H.; Sivel, V.G.M.; de Wit, J.H.W. Changes in epoxy-coated aluminium due to exposure to water. *Prog. Org. Coat.* **2004**, *51*, 351–364. [[CrossRef](#)]
44. Vellinga, W.P.; Eising, G.; de Wit, F.M.; Mol, J.M.C.; Terryn, H.; de Wit, J.H.W.; De Hosson, J.T. Adhesion at Al-hydroxide-polymer interfaces: Influence of chemistry and evidence for microscopic self-spinning. *Mater. Sci. Eng. A* **2010**, *527*, 5637–5647. [[CrossRef](#)]
45. Rider, A.N.; Brack, N.; Andres, S.; Pigram, P.J. The influence of hydroxyl group concentration on epoxy-aluminium bond durability. *J. Adhes. Sci. Technol.* **2004**, *18*, 1123–1152. [[CrossRef](#)]
46. Van den Brand, J.; Snijders, P.C.; Sloof, W.G.; Terryn, H.; de Wit, J.H.W. Acid-base characterization of aluminium oxide surfaces with XPS. *J. Phys. Chem. B* **2004**, *108*, 6017–6024. [[CrossRef](#)]
47. Van den Brand, J.; Van Gils, S.; Beentjes, P.C.J.; Terryn, H.; de Wit, J.H.W. Ageing of aluminium oxide surfaces and their subsequent reactivity towards bonding with organic functional groups. *Appl. Surf. Sci.* **2004**, *235*, 465–474. [[CrossRef](#)]
48. Yang, C.; Xing, X.; Li, Z.; Zhang, S. A comprehensive review on water diffusion in polymers focusing on the polymer-metal interface combination. *Polymers* **2020**, *12*, 138. [[CrossRef](#)] [[PubMed](#)]